Received: 27 May 2016 | Revised: 21 July 2016 | Accepted: 22 July 2016

DOI 10.1002/bip.22925

ORIGINAL ARTICLE

WILEY Biopolymers

Ocellatin-PT antimicrobial peptides: High-resolution microscopy studies in antileishmania models and interactions with mimetic membrane systems

Mayara Oliveira[1,2] | Ana Georgina Gomes-Alves[3,4,5] | Carla Sousa[2] | Mariela Mirta Marani[6] | Alexandra Plácido[7] | Nuno Vale[2] | Cristina Delerue-Matos[7] | Paula Gameiro[2] | Selma A. S. Kückelhaus[1,8] | Ana M. Tomas[3,4,9] | José Roberto S. A. Leite[2,8,10] | Peter Eaton[2,10]

[1] Programa de Pós-Graduação em Medicina Tropical, Núcleo de Medicina Tropical, NMT, Faculdade de Medicina, Universidade de Brasília, Brasília, DF, Brazil

[2] Instituto de Investigação e Inovação em Saúde, Universidade do Porto, Porto 4200, Portugal

[3] IBMC, Instituto de Biologia Molecular e Celular, Universidade do Porto, Porto, Portugal

[4] UCIBIO, REQUIMTE, Departamento de Química e Bioquímica, Faculdade de Ciências, Universidade do Porto, Porto, Portugal

[5] CEB, Centro de Engenharia Biológica, Universidade do Minho, Campus de Gualtar, Braga 4710-057, Portugal

[6] PEEC – CONICET, Consejo Nacional de Investigaciones Científicas y Técnicas, Puerto Madryn, Chubut, Argentina

[7] REQUIMTE/LAQV, Instituto Superior de Engenharia do Instituto Politécnico do Porto, Porto, Portugal

[8] Departmento de Morfologia, Faculdade de Medicina, Universidade de Brasília, Brasilia, Brazil

[9] ICBAS, Instituto de Ciencias Biomedicas Abel Salazar, Universidade do Porto, Porto, Portugal

[10] Núcleo de Pesquisa em Biodiversidade e Biotecnologia, Biotec, Campus Ministro Reis Velloso, Universidade Federal do Piauí, UFPI, Parnaiba, PI, Brazil

Correspondence
Peter Eaton, UCIBIO, REQUIMTE, Departamento de Química e Bioquímica, Faculdade de Ciências da, Universidade do Porto, Rua do Campo Alegre, 687, Porto 4169-007, Portugal.
Email: peter.eaton@fc.up.pt

Abstract

Although the mechanism of action of antimicrobial peptides (AMPs) is not clear, they can interact electrostatically with the cell membranes of microorganisms. New ocellatin-PT peptides were recently isolated from the skin secretion of *Leptodactylus pustulatus*. The secondary structure of these AMPs and their effect on *Leishmania* infantum cells, and on different lipid surface models was characterized in this work. The results showed that all ocellatin-PT peptides have an α-helix structure and five of them (PT3, PT4, PT6 to PT8) have leishmanicidal activity; PT1 and PT2 affected the cellular morphology of the parasites and showed greater affinity for leishmania and bacteria-mimicking lipid membranes than for those of mammals. The results show selectivity of ocellatin-PTs to the membranes of microorganisms and the applicability of biophysical methods to clarify the interaction of AMPs with cell membranes.

KEYWORDS

Antimicrobial peptides, atomic force microscopy, scanning electron microscopy, Leishmania infantum, lipid membranes, surface plasmon resonance

1 | BACKGROUND

Antimicrobial peptides (AMPs) are ubiquitous naturally occurring molecules forming part of many species' innate immune system. They have between 12 and 50 residues and most of them are cationic-amphipathic molecules often with a high content of α-helix in their structure.[1] Antibacterial activity is the most commonly tested antimicrobial activity for AMPs, however many other activities have also been described.[2] Regarding antiparasitic activity of AMPs, only 83 of more than 990 active peptides derived from amphibians registered at APD have been tested as antiparasitic, mostly having been tested for antimalaria activity.[3] Furthermore, no correlation between antibacterial and antiparasitic activity potencies was observed in those AMPs that have been tested.[4] Antimicrobial peptides have potential to form a new class of molecules able to treat neglected diseases, including those caused by parasites.[5] Although the mechanisms of action of AMPs against parasites are not fully understood, it has been demonstrated that generally, AMPs kill target cells by disrupting the cell membranes.[6]

High-resolution microscopy techniques are powerful tools to observe the effect of antimicrobial agents on the morphology of microorganisms with resolutions on the order of a few nanometers to fractions of nanometers.[7] Both scanning electron microscopy (SEM) and atomic force microscopy (AFM) give information about sample surface topography.

AFM allows sample observation under ambient conditions, with no requirement for a conductive coating. Moreover, AFM permits the quantification of roughness of membranes. Compared to AFM, SEM requires more complex sample preparation procedures for biological samples since it's a vacuum technique, but is more appropriate for characterizing large numbers of cells, since the field of view can be wider, and imaging is considerably faster.

The effects of AMPs observed on the surface structure of microorganisms can be related to their affinities to the lipid composition of the membrane: prokaryotic and eukaryotic membranes vary considerably in lipid contents. Anionic lipids are exposed at the surface of many bacterial membranes, while in eukaryotic membranes contain very low concentrations of anionic lipids. Phosphatidylethanolamine (PE) is present at high concentration in many bacteria specie surfaces, while in mammalian cells, this lipid makes up less than 5% of the surface lipid composition. Several studies show the increasing role of PE as a lipid receptor in the action of AMPs (reviewed in Ref. 8). Phosphatidylglycerol (PG) is another of the essential components of bacterial cell membranes, which confers a negative charge at physiological pH and has a role is providing bacterial membrane stability.[9] Overall, PE and PG make up a great proportion of the lipid contents of the *E. coli* inner membrane.[10] In the case of parasites, a number of studies demonstrate that phosphatidylcholine (PC) and PE are the two most abundant phospholipid classes in the membrane of some species, including Leishmania.[11] Surface plasmon resonance (SPR) is a useful tool for studying membrane affinity of small molecules. This technique can be used to measure the interaction of peptides with different synthetic lipid bilayer models.[12] In this work, dimyristoylphosphatidylcholine (DMPC) is used as a model for eukaryotic membranes while POPE:POPG (75:25) and POPC:POPE (75:25) are used as models for *E. coli* and parasite membranes, respectively. These first two have been used by other authors as models for these classes of cell,[9a,13] while to our knowledge no work on model membranes of *Leishmania* has been carried out.

Recently we isolated eight new AMPs from the skin secretion of *Leptodactylus pustulatus*. They belong to the ocellatin peptide family found in the genus *Leptodactylus*. The first member of this family, ocellatin-1, was described in the specie *Leptodactylus ocellatus*,[14] then 23 more peptides were described with similarities in amino acid sequence in seven species of the same genus.[14,15] This family of peptides was predicted to have an amphipathic α-helix secondary structure and they possess in general low potency against Gram-negative tested strains and no activity or higher MICs for Gram-positive strains.

However no biological effects other than bacterial growth inhibition have been described for ocellatin peptides except for plasticin-L1 that presented a modest insulin-releasing effect when tested *in vitro*[16] and leptoglycin and ocellatin-F (fallaxin) that were tested against human pathogenic fungi but did not show any growth inhibition.[17] In this work we characterized the secondary structure of ocellatin-PT peptides by circular dichroism (CD) and we evaluated their effect in vitro in *Leishmania infantum* (= *L. chagasi*) cultures, by high-resolution microscopy techniques (AFM and SEM), and on different lipid systems by SPR.

2 | METHODS

2.1 | Peptide synthesis and characterization

All of the peptides were manually synthesized using a solid-phase approach using F-moc/tert-butyl chemistry. Peptide elongation was carried out in polypropylene syringes fitted with a polyethylene porous disk. Solvents and soluble reagents were removed by suction. A Wang resin (Peptides International) was used for the synthesis of the peptides, except when the amidated N-terminal peptides were produced, for which a Rink amide MBHA resin (Peptides International) was used. Samples were treated with trifluoroacetic acid/triisopropylsilane/water (TFA/TIS/H2O) (95:2.5:2.5) for removal of the protecting group. Peptide purification was

carried out by preparative RP-HPLC (Phenomenex columns Kinetex 5 μm C18 50 × 21.20 mm) using a Shimadzu Prominence instrument. Each peptide was dissolved in H_2O/CH_3CN (6:4) and submitted to an RP-HPLC system using a gradient of CH_3CN, starting with H_2O/0.1% TFA and rising to 100% CH_3CN over 15 minutes.[15a] The formula $(A_{215} - A_{225}) \times 144$ (μg/mL) was applied for peptide quantification.[18] Purity and molecular mass determination of synthetic peptides were performed using a MALDI-TOF/TOF (UltrafleXtreme, Bruker Daltonics) instrument operated in the positive ion mode and controlled by the Compass for Flex software, version 1.3 (FlexControl 3.3, FlexAnalysis 3.3, Bruker Daltonics); 5,000 laser shots were accumulated per spectrum in the MS and MS/MS modes. One-microliter aliquots of the chromatographic fractions dissolved in an α-cyano-4-hydroxycinamic acid matrix solution (1:3, v/v) were applied on a stainless steel plate and dried at room temperature for 30 minutes. The peptide monoisotopic mass was obtained in reflector mode with external calibration, using the Peptide Calibration Standard for Mass Spectrometry mixture (up to 4000 Da mass range, Bruker Daltonics). Isolated peptides were submitted to an automatic sequencer for *de novo* sequencing using LIFT mode.[15a] All peptides synthesized and used in this study are shown in Supporting Information Table S1. All peptides synthesized as well as some physico-chemical characteristics relevant as isoelectric point[19] and GRAVY (Grand Average of Hydropathy)[20] are shown in Supporting Information Table S1.

All peptides synthesized and used in this study were obtained at >99% purity by HPLC. The molecular weights were determined as: Ocellatin-PT1 (Mw 2639.1; $[M + H]^+ = 2638.24$ Da), Ocellatin-PT2 (Mw 2609; $[M + H] + = 2607.68$ Da), Ocellatin-PT3 (Mw 2530; $[M + H]^+ = 2528.53$ Da), Ocellatin-PT4 (Mw 2595.1; $[M + H]^+ = 2593.46$ Da), Ocellatin-PT5 (Mw 2667.1; $[M + H]^+ = 2666.45$ Da), Ocellatin-PT6 (Mw 3364.9; $[M + H]^+ = 3365.74$ Da), Ocellatin-PT7 (Mw 3293.8; $[M + H]^+ = 3293.69$ Da), Ocellatin-PT8 (Mw 3312.9; $[M + H]^+ = 3312.71$ Da). All the mass spectrometry data are published in the supporting information of the article.[13]

2.2 | Antileishmania assays

Parasite cultures. *Leishmania infantum* promastigotes (MHOM MA67ITMAP263) were cultured at 25°C in RPMI 1640 Glutamax (Gibco) supplemented with 10% (v/v) iFBS, 50 U mL^{-1} penicillin, 50 μg/mL streptomycin, and 20 mM HEPES sodium salt pH 7.4 (Sigma). Axenic amastigotes of the same strain were grown at 37°C and 5% CO_2, in MAA medium supplemented with 20% (v/v) iFBS, 2 mM Glutamax (Gibco), and 0.023 mM hemin (Sigma), as described previously.[21]

2.3 | Assessment of leishmanicidal activity

For determination of the leishmanicidal activity of the peptides, *L. infantum* parasites at late exponential phase of growth were placed in 96-well plates: (i) promastigotes were seeded at 3×10^5 cells per well in complete RPMI medium, (ii) axenic amastigotes were seeded at 1.5×10^5 cell per well in MAA20. Parasites were exposed to different concentrations of peptides for 24 h. Parasite viability was then determined by the resazurin assay[22] and calculated as the percentage in relation to control cultures. Data were analyzed with GraphPad Prism 5 software and IC_{50} values determined.

2.4 | Generation of bone-marrow derived macrophages (BMDM)

Bone-marrow (BM) cells were isolated by flushing femurs and tibia of BALB/c mice with Hank's Balanced Salt Solution (HBSS, Gibco), and differentiated into BM derived macrophages (BMDM) *via* an adaptation of a previously described protocol.[23] Briefly, BM cells were collected, centrifuged and suspended in Dulbecco's Modified Eagle's Medium (DMEM) supplemented with 10% inactivated Fetal Bovine Serum (iFBS), 1% of Minimum Essential Media non-essential amino acids solution (MEM), 50 U.mL^{-1} penicillin, 50 μg/mL streptomycin (all from Gibco) (complete DMEM medium or cDMEM), and 10% L929 cell conditioned medium (LCCM) as a source of macrophage-colony stimulating factor (M-CSF). BM cells were cultured in petri dishes for 24 h at 37°C in a 7% CO_2 atmosphere in order to remove differentiated cells. Non adherent cells were then counted, plated in 96-well plates (2.5-3 × 10^4 cells per well) and incubated at 37°C in a 7% CO_2 atmosphere. On the 4th and 7th day, cDMEM + 10% LCCM medium was renewed. After 10 days the culture was composed of differentiated macrophages.

2.5 | Assessment of cytotoxicity to BMDM

Cytotoxicity of peptides was determined in BMDM using a standard resazurin assay.[22] Cultures of BMDM were supplemented with different concentrations of the test compounds and further incubated for 24 h. Then, 10% (v/v) of a 2.5 mM resazurin solution (Sigma) was added to each well. Cells were incubated for 2 h and fluorescence measured ($560_{Ex}/590_{Em}$) using a SpectraMAX GeminiXS microplate reader (Molecular Devices LLC). The percentage of viable BMDM was calculated in relation to control cultures to which no peptides were added. Data were analyzed with GraphPad Prism 5 software and 50% cytotoxic concentration (CC_{50}) values determined.

2.6 | Circular dichroism studies

We studied the secondary structure content by CD spectroscopy in the far UV, using a Jasco J-815 CD Spectropolarimeter (Jasco Corp.). The measurements were performed under nitrogen gas flow of 8 L/hour at a temperature of 20°C, controlled by a Peltier system (JASCO). Spectra were recorded between 190 and 260 nm, using a 10 mm cell path length. The peptide concentrations were 100 μM and the 2,2,2-Trifluoethanol (TFE) concentrations were 0%, 10%, 20% and 40% (v/v) in Milli-Q water. For the studies using liposomes, the LUVs (for preparation details see below) were used at a lipid concentration of 1 $mMdm^{-3}$, and peptides were used at 100 μM concentration. These experiments were carried out at a controlled temperature of 37°C, and other conditions were the same as for the TFE studies. In order to reduce the interference by light scattering from the vesicles, a reference spectrum of a solution containing only LUVs in buffer, with no peptide was used as a background and subtracted from the spectra before plotting and before analysis. We used a scan speed of 50 nm/min, a response time of 1 s and a bandwidth of 1 nm. The spectra were converted to molar ellipticity per residue by using the relationship: $[\theta]/\theta(10 \times c \times n \times d)$, here $[\theta]$ is the molar ellipticity (in degrees × cm^2 × $dmol^{-1}$), θ the ellipticity in millidegrees, n is the number of peptide bonds and c its molar concentration, d the length of the cell in centimeters. Helicity content estimates were calculated using the Dichroweb online service,[24] using the CONTIN-LL method.[25]

2.7 | Morphological studies using SEM and AFM

To evaluate the morphological effects resulting from treatment with ocellatin-PT peptides, we select two of the eight peptides, to represent both ocellatins size classes used in this study. Ocellatin-PT1 represents those with small size (25 residues) and ocellatin-PT8 represents large size peptides (31 residues). These peptides were also selected because of their low cytotoxicity to mammalian cells.

We used a 96 well microculture plate with 100 μL of RPMI 1640 per well, to which were added 2×10^6 promastigote forms per well, in triplicate. Three conditions were studied: a negative control (no peptide), a sample treated with ocellatin-PT1 or ocellatin-PT8 at the concentration of 16 μg/mL and 64 μg/mL. Plates were incubated at 37°C for 24 h. Cultures were transferred to tubes and were centrifuged at 100 × g for 15 minutes. Culture medium was removed and a wash with sodium cacodylate buffer was performed (5 minutes, 100 mM; pH 7.2), after buffer removal a primary fixation with glutaraldehyde solution (60 minutes, 2.5% in 100 mM Na-cacodylate, pH 7.2) was made. After this time, two buffer washes were made to remove glutaraldehyde. The cells were then transferred to poly-L-lysine-treated glass slides (10 mm diameter) and they were left to settle for 60 minutes. Later, the samples were washed (twice) with ultrapure water, and slides were covered with osmium tetroxide solution (at 4° C, 1% in 100 mM Na-cacodylate buffer, pH 7.2) for secondary fixation. After this, the osmium tetroxide solution was removed by ultrapure water wash, and then the samples were treated with a graded ethanol series for dehydration (25, 50, 75, and 100% twice, 5 minutes each). Finally, the samples in 100% ethanol were transferred to a critical point drying (CPD) device. After CPD the samples were maintained in a dry environment. The samples were then divided in two. One set of these samples were subjected to Au/Pd coating before SEM analysis; the other set of samples was used for AFM analysis without further treatment.

SEM was performed using a FEI Quanta FEG 400 scanning electron microscope. Images were collected in both secondary electron (SE) and (BSE) imaging modes. Typical imaging conditions were 15 kV acceleration, and 10-12 mm working distance; spot size and aperture were adjusted to achieve the best possible resolution. Many areas were imaged per sample, representative images are shown.

AFM was performed with a TT-AFM atomic force microscope from AFMWorkshop. A 50 × 50 × 17 μm scanner was used, in vibrating mode. ACT probes from AppNano were used with resonance frequencies of approximately 300 kHz. Images were processed and displayed using Gwyddion software, which was also used to calculate RMS roughness (Rq) of central areas of membranes of the parasites. A p value of <0.05 was considered to be significant.[7a]

2.8 | Liposome preparation

2.8.1 | Liposome preparation

Lipid films were prepared by evaporation of a lipid solution in chloroform using a stream of argon. The lipids POPE, POPG, POPC and DMPC were weighed in order to have final stock lipid dispersions (POPE:POPG (75:25); POPC: POPE (75:25); DMPC) with 2 $mmol \cdot dm^{-3}$. The films were left under vacuum for 3 h to remove all traces of the organic solvent. Resulting dried lipid films were dispersed with HEPES buffer (0.1 M NaCl, pH 7.4) then the mixture was vortexed above the phase transition temperature of the lipid (40 ± 0.1°C used for all lipid systems studied) to produce multilamellar large vesicles (MLVs). The MLVs were processed by five cycles of freezing in liquid nitrogen and thawing by brief immersion in a boiling water bath. Lipid suspensions were then equilibrated above the phase transition temperature of the lipid for 30 min and extruded 10 times through 100 nm polycarbonate filters to produce large

TABLE 1 Antileishmania activity against *Leishmania infantum* and cytotoxicity of Ocellatins

Peptides	IC_{50} (μg/mL/μmol.dm^{-3}) Promastigotes	IC_{50} (μg/mL/μmol.dm^{-3}) Axenic Amastigotes	Cytotoxicity CC50 (μg/mL) bone marrow-derived macrophages (BMDM) macrophages
Ocellatin-PT1	63.4/23.9	NAD[a]	> 512
Ocellatin-PT2	≫128/≫ 49.1	NAD	> 512
Ocellatin-PT3	34/13.4	NAD	> 512
Ocellatin-PT4	25.6/9.8	75/28.9	263.4
Ocellatin-PT5	62.7/25.5	NAD	> 512
Ocellatin-PT6	42.6/12.7	67.5/19.8	> 512
Ocellatin-PT7	42.2/72.8	NAD	> 512
Ocellatin-PT8	51.6/15.5	NAD	> 512

[a]No activity was detected at the highest antibiotic concentration tested.

unilamellar vesicles (LUVs). Extrusion of the liposomes was performed using a LIPEX Biomembranes extruder attached to a thermostatic circulating water bath. The size distribution of the LUVs was determined by dynamic light scattering (DLS) analysis using a Malvern Instruments ZetaSizer Nano ZS and the hydrodynamic diameters are listed in Supporting Information Table S2.

2.9 | SPR measurements

SPR experiments were carried out using a Biacore X100 analytical system with a L1 sensor chip (Biacore). Prior to use, the L1 chip surface was washed with a conditioning cycle consisting on the injection of 3-[(3-cholamidopropyl)dimethylamonio]-1-propanesulfonate (CHAPS), 20 mmol.dm^{-3} followed by running buffer (HEPES). The interaction of the ocellatins-PT1 and PT8 with the lipid models was examined at peptide concentrations of 0, 2, 3, 4, and 5 μmol.dm^{-3} and a distinct SPR cycle was performed for each peptide concentration tested. Three types of vesicles were tested: DMPC, POPC:POPE (75:25), and POPE:POPG (75:25). Each SPR cycle consisted of vesicle immobilization on the chip surface with an injection of the 1 mmol.dm^{-3} LUV suspension, at a flow rate of 2 μl/min for 45 min. This was followed by successive injections of running buffer (50 μl/min for 100s) and 1 mmol.dm^{-3} NaOH (50 μl/min for 60 s). Stabilization finished with an injection of running buffer at 5 μl/min for 500 s. After stabilization, peptide solution was injected at a flow rate of 10 μl/min during 100 s followed by a dissociation time of 10 min (Supporting Information Figure S1). Then the lipids were removed by a double injections of CHAPS and running buffer, both at a flow rate of 10 μl/min for 150 seconds. The running buffer was 20 mM phosphate buffer pH 7.4, 150 mM NaCl. Kinetic analysis of the sensorgrams was performed using the two-state curve fitting model.

3 | RESULTS

3.1 | Biological assays

In this work, we analyzed the biological activity of eight ocellatin-PT peptides against *L. infantum* promastigotes and amastigotes and their cytotoxicity to bone marrow-derived macrophages (BMDM).

Anti-parasitic activity of PT3, PT4, PT6, PT7, and PT8 eliminated half of the promastigote population (Table 1 and Supporting Information Figure S2) at concentrations between 9.8 and 15.4 μM, while 50% inhibitory concentrations (IC_{50}) of ocellatins PT1, PT2 and PT5 were 24, 49 and 26 μM. Amastigotes were more resistant to the action of these AMPs, the most effective being Ocellatin-PT6 and PT4 that showed (IC_{50} of 19.8 and 28.9 μM, respectively (Table 1 and Supporting Information Figure S3). None of the other peptides had a detectable effect on the amastigotes in the concentration range tested.

As depicted in Table 1 and Supporting Information Figure S4, the cytotoxicity of the AMPs toward our mammalian cell model, bone marrow-derived macrophages (BMDM), was in general low. All the peptides presented 50% cytotoxicity concentrations (CC_{50}) superior to the highest concentration tested, 150 μM (>512 μg/mL) with the exception of PT4 that had a CC_{50} of 101.5 μM.

3.2 | STRUCTURAL STUDIES

Ocellatin-PT secondary structures were studied using CD spectroscopy both in the absence and presence of increasing amounts of TFE, and selected peptides were further probed in the presence of the three membrane models used in this work, namely DMPC—the mammalian cell membrane mode), POPE:POPG (75:25)—Gram negative bacterial cell

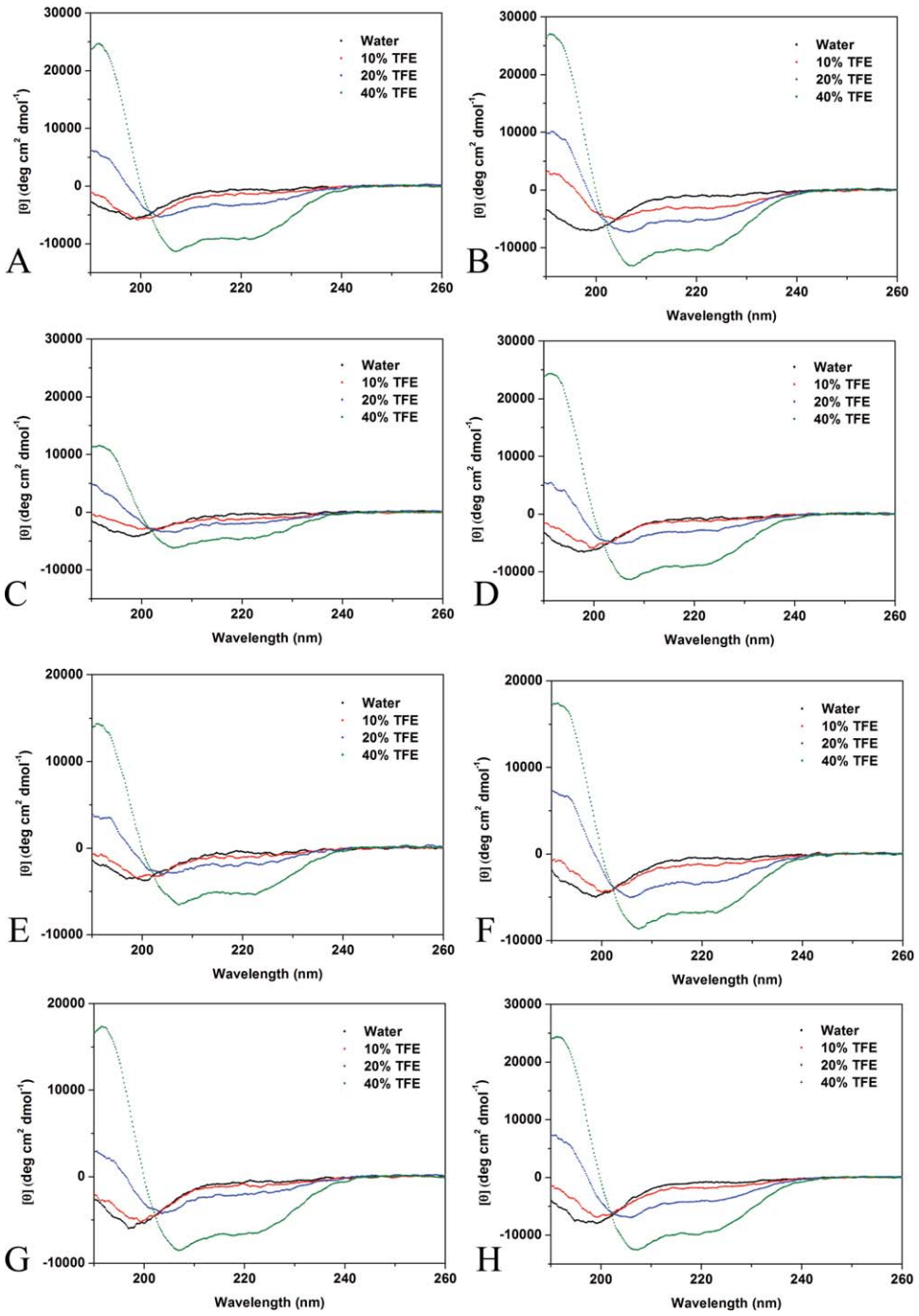

FIGURE 1 Circular dichroism of peptides in aqueous solution and in 2,2,2-TFE. (**A**) Ocellatin-PT1, (**B**) Ocellatin-PT2, (**C**) Ocellatin-PT3, (**D**) Ocellatin-PT4, (**E**) Ocellatin-PT5, (**F**) Ocellatin-PT6, (**G**) Ocellatin-PT7, and (**H**) Ocellatin-PT8

membrane model, and POPC:POPE (75:25)—the cell membrane model for leishmania. CD studies were performed in order to be compared with the three-dimensional structural models of ocellatin-PT peptides previously described using the web resource PEP-FOLD[19]. Three-dimensional structure predictions previously described showed two similar α–helix structures in all Ocellatin-PT peptides: one smaller at the N-terminal that covered residues 1 to 8 separated by a small random coil from a bigger α–helix that covered 11–20 residues. Predicted models showed small differences probably due to some residue differences between peptides[19]. CD measurements of ocellatin-PT peptides in water and 10% of TFE indicate a random conformation with a minimum close to 198 nm (Figure 1). However as TFE concentration increases, the shape of CD spectra suggest the tendency to form defined secondary structures. All CD spectra at 40% TFE showed one maximum at 191 nm and two minima around 207 and 220 nm characteristic of α–helix structures

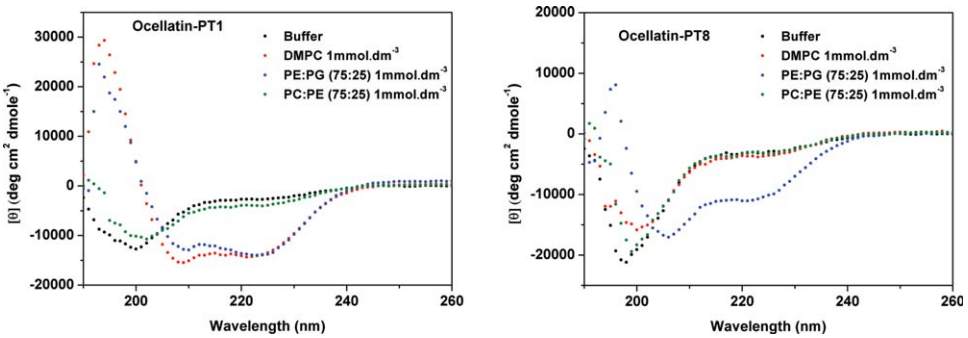

FIGURE 2 Circular dichroism of peptides in buffer (PBS) and in solutions (all 1mM) of LUVs in the same buffer. Left: Ocellatin-PT1, Right: Ocellatin-PT8

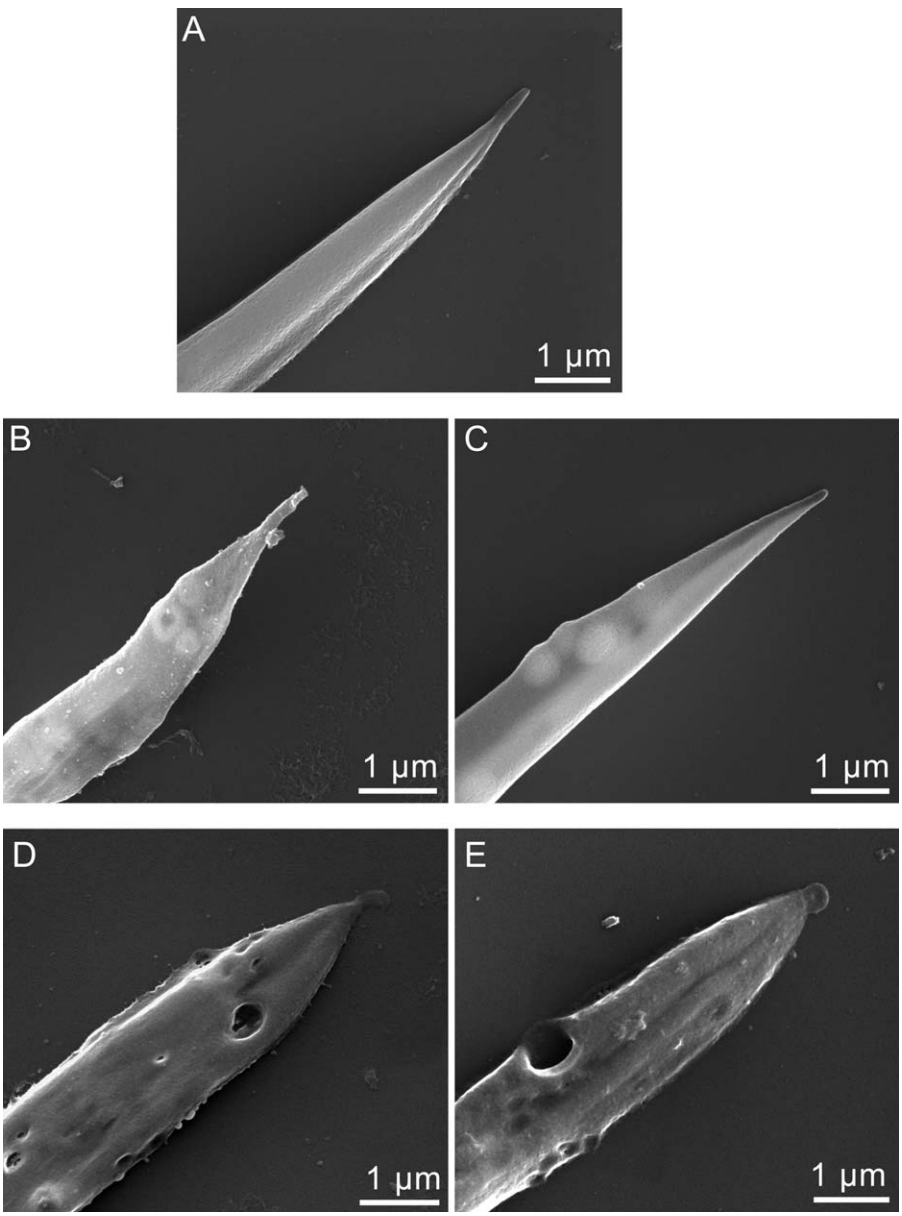

FIGURE 3 Scanning Electron Microscopy imaging of *L. infantum* promastigote forms. (**A**) Control cell. (**B**) Cell treated with 16 µg/mL of ocellatin-PT1. (**C**) Cell treated with 16 µg/mL of ocellatin-PT8. (**D**) Cell treated with 64 µg/mL of ocellatin-PT1. (**E**) Cell treated with 64 µg/mL of ocellatin-PT8. All images are SE images

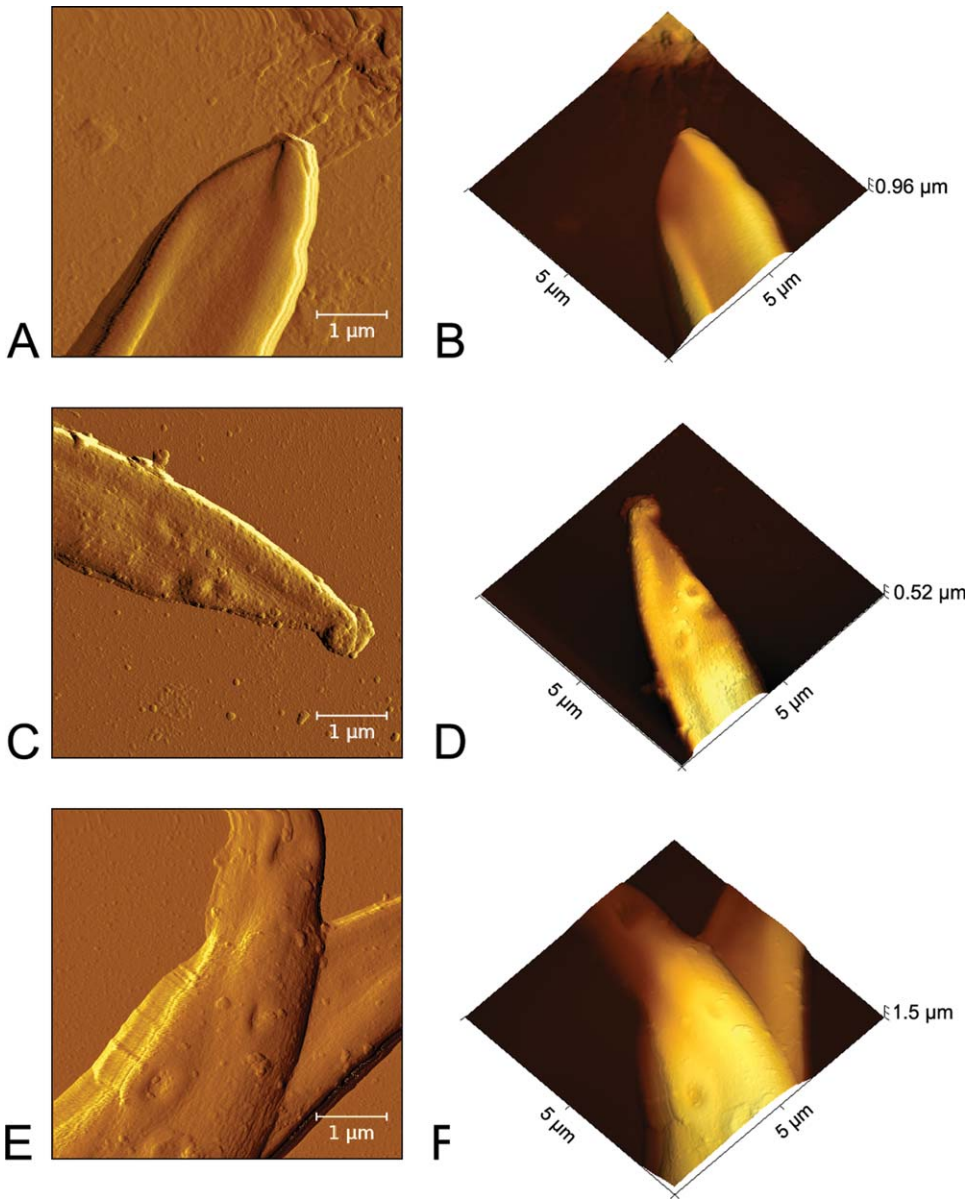

FIGURE 4 Atomic force microscopy images of *L. infantum* promastigote forms. Control cell: (**A**) Amplitude image and (**B**) 3D representation of height image of the same control cell. A cell treated with 16 µg/mL of Ocellatin-PT1: (**C**) Amplitude image and (**D**) 3D representation of height image of the same treated cell. A cell treated with 16 µg/mL of Ocellatin-PT8: (**E**) Amplitude image and (**F**) 3D representation of height image of the same treated cell

(Figure 1). Estimated helical contents were calculated and the results included in the supporting material (Supporting Information Table S3). The estimated helicities varied form peptide to peptide, being as low as ca. 17% for Ocellatin PT-3, to over 38% for Ocellatin PT-8. However, all peptides showed increased helicity with increasing TFE concentration. This data correlates with the results obtained for plasticin-L1, the only one of the 23 AMPs isolated from the skin secretion of frogs from the genus Leptodactylus that has been previously studied by CD[21]. Plasticin-L1 CD spectra showed a helical structure when dissolved in 50% TFE, but not when dissolved in water or methanol[21]. This solvent-dependent structure adoption could indicate that these peptides are unstructured until interaction with microorganism membranes, as was previously demonstrated for AMPs of other species.

In order to test this hypothesis, we also tested the CD response of two selected peptides (ocellatins PT-1 and PT-8) to the presence of lipid membranes in the form of LUVs. These two peptides were chosen as representing different properties of the peptides within this class, Ocellatin–PT1 being a shorter peptide with relatively low charge (25 residues, pI of 8.44) while Ocellatin–PT8 is the longest peptide in the group and highly cationic (32 residues, pI of 9.82). They were tested against LUVs made up of DMPC, POPE:POPG (75:25) and POPC:POPE (75:25). Results are shown

in Figure 2, and estimated helicity percentages are reported in Supporting Information Table S4. The results show environment-dependent structural changes in the peptides, confirming the results shown with the TFE. The results however, were somewhat more complex. Overall, while we saw increases in helicity when the peptides were solutions containing lipid vesicles, the amount of secondary structure depended strongly on the peptide studied and the type of lipid in the vesicle. Both peptides studied developed alpha helical character in the presence of the bacterial membrane-mimicking model (POPE:POPG), but to a lesser extent, in the case of leishmania membrane model (POPC:POPE). Furthermore, in the case of the DMPC, the peptide Ocellatin-PT1 developed considerable helical content, while the Ocellatin PT-8 peptide did not. This contrast with cytotoxicity results reported here (Supporting Information Figure S4), and previously,[15a] showing no difference between these peptides in terms of cytotoxicity toward mammalian cells.

3.3 | Morphological studies

SEM and AFM were used to generate high-resolution microscopy data on morphological alterations caused by the ocellatins under study on *L. infantum* promastigote forms. Both techniques complement each other. AFM is a rather slow high-resolution imaging technique that enables texture analysis of the membranes, while SEM's speed and wide field imaging allow an overview of the variety in morphology of the cells. Typically for each sample, more than 20 cells were scanned with SEM, while 4-6 cells were examined with the AFM. This complementarity between SEM and AFM imaging has been exploited by us to examine peptide-treated *Leishmania* promastigotes previously.[26] Representative images from both techniques are shown (Figures 3 and 4).

Examining the SEM images, considerable changes in the membranes of the parasite body upon treatment with the peptides was observed (Figure 3). Both ocellatin-PT1 and ocellatin-PT8 has similar effects. At the 16 μg/mL peptide concentration (Figures 3B and 3C), the cells showed several raised circular features, consistent with large vesicles in the membrane. The images shown in Figure 3 are SE images. Backscattered electron (BSE) images, acquired simultaneously are shown in the supporting information (Supporting Information Figure S5). BSE images are less surface sensitive, and show more information from deep within the sample. The BSE images revealed even more circular features (presumably vesicles), as well as dark patches perhaps reflecting areas of the membranes that had undergone membrane thinning.[27] These features were largely absent from control cells (see Figure 3A). After treatment at 64 μg/mL (Figures 3D and 3E), the cells were further altered, the raised "blister-like" swellings being replaced with what are apparently deep holes in the cell body. In some cases, the appearance of these holes gave the impression that the cell had undergone lysis, while at 16 μg/mL, alterations were mostly limited to vesicle appearance and collapse. In the BSE images (Supporting Information Figure S5), dark patches were sometimes observed along the membrane, as well as more hole-like alteration as observed in the SE images. In previous work it was observed that the shape of the cells changed upon treatment with the AMP DRS-01, becoming more rounded and significantly shorter overall.[26] In this work, we did not notice gross morphological changes of this type in the images (see Figure 3 where the overall shape of the cells does not change). Using lower magnification images, we measure the length of the cell bodies, for the cells treated with 16 μg/mL and found there were small but non-significant changes in cell length. Control cells measured 9.6 ± 2.2 ($N = 21$), while Ocellatin PT-1-treated cells measured 8.4 ± 1.3 μm ($N = 7$), and Ocellatin PT-8-treated cells measured 8.3 ± 2.2 μm ($N = 14$).

Samples treated with 16 μg/mL peptide were also examined with AFM. These samples were treated in parallel with the SEM samples, but neither metal-coated nor exposed to vacuum. The lack of metal coating allows texture analysis without interference from metal grains from the sputtering procedure, and not exposing the cells to vacuum removed the possibility of vacuum-induced morphological changes. The images shown in Figure 4 largely show similar effects to those seen in the SEM samples. Circular features (sometimes collapsed in the center) in the two treated samples indicated the presence of blister-like features. Examination of the cell surface images from the AFM results showed a change in texture over the whole membrane in the treated sample compared to the control. Measurement of roughness was

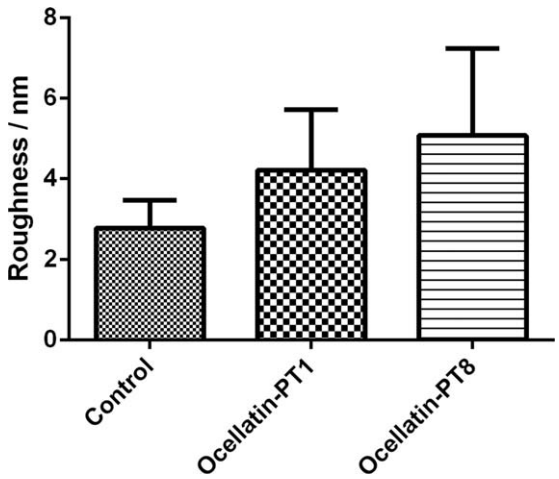

FIGURE 5 Surface roughness (Rq) measured by AFM on the surface of promastigote forms of *L. infantum* cells. Raw values were 2.78 nm (SD: 0.63, *N*: 25) for the control, 4.22 nm (SD: 1.50, *N*: 22) for treatment with Ocellatin-PT1, and 5.08 (SD: 2.16, *N*: 18) for treatment with Ocellatin-PT8

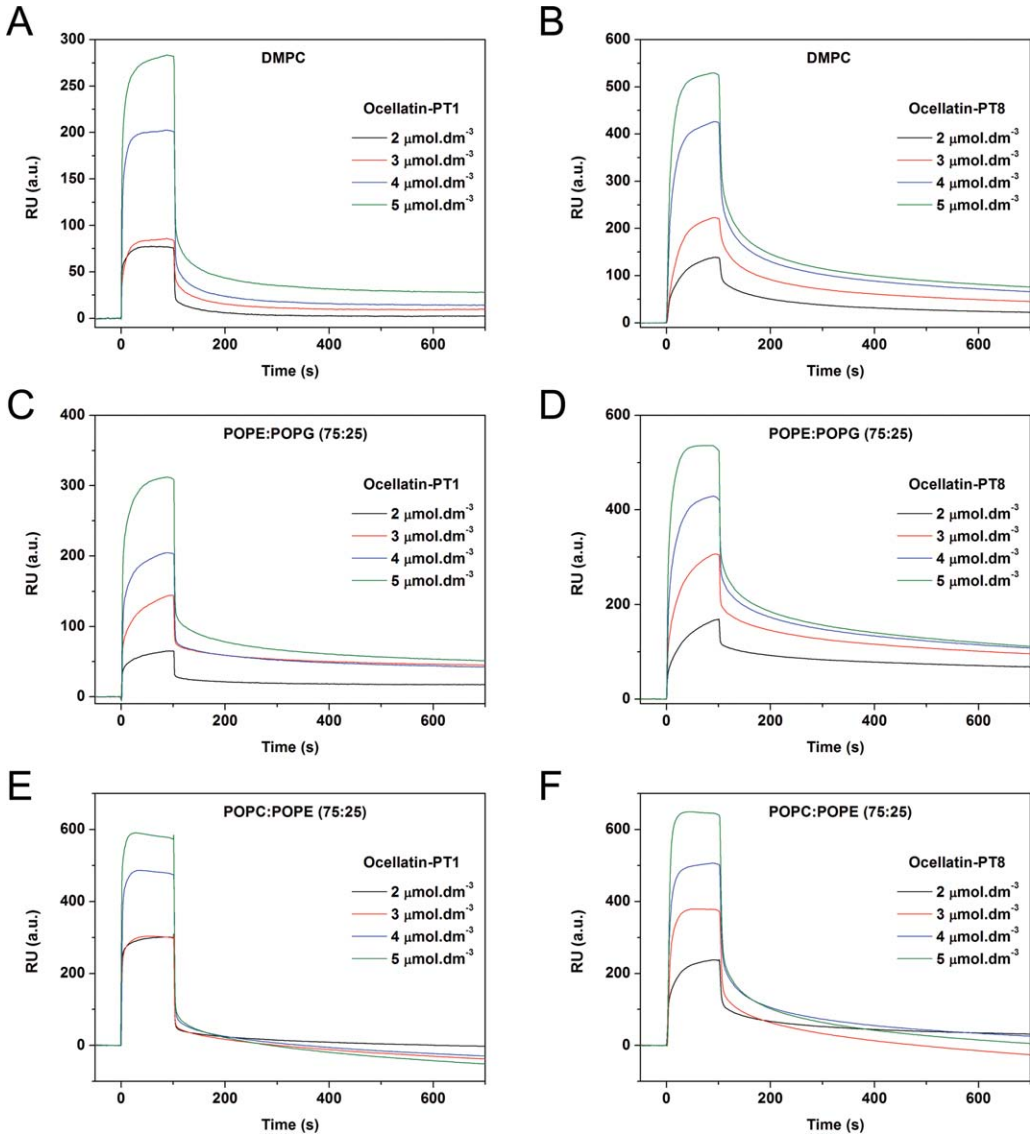

FIGURE 6 Representative SPR sensorgrams obtained for Ocellatin-PT1 and Ocellatin-8 binding to mimetic model membranes. (**A**) and (**B**) DMPC supported unilamellar bilayers. (**C**) and (**D**) POPE:POPG (75:25) supported unilamellar bilayers. (**E**) and (**F**) POPC:POPE (75:25) supported unilamellar bilayers at four different peptide concentrations ranging from 2–5 μM. Injections of peptide occurred between $t = 0$ and $t = 100$ and the peptide was then allowed to dissociate for a further 600 seconds (between $t = 100$ and $t = 700$ seconds) as buffer flowed through the system

performed along the center of the cell membranes in treated and untreated cells. All cells imaged were measured, and the results averaged (Figure 5). The averages for both cells treated with ocellatin-PT1 and -PT8 were higher than the control cells. Further, the roughness of ocellatin-PT8-treated cells was higher than that found after treatment with ocellatin-PT1, although the difference was slight. In fact, the standard deviation was quite large for all of these measurements. This is not surprising, since the treated cells were quite heterogeneous, and biological cells vary quite a lot in roughness. Presumably due to the large variability in surface texture, the results failed the Student's *t*-test for statistical significance ($p > .05$), nevertheless suggest an overall change in membrane texture upon treatment.

3.4 | Binding property of peptides to lipid membranes

The binding of the ocellatins PT-1 and PT-8 to lipid model membranes was explored using SPR. DMPC, POPC:POPE (75:25) and POPE:POPG (75:25) liposomes were used to mimic mammalian, leishmania and bacteria membranes, correspondingly. At the higher concentrations of peptide used, the decrease of the SPR signal clearly showed that the lipid bilayer was affected by the peptide. In fact, lipid bilayers were very unstable at high concentrations of the peptide, making measurements unreliable. Therefore, we used separate cycles of lipid deposition for each peptide concentration tested. Supporting Information Figure S1 depicts an example of an SPR experiment cycle, showing the deposition of the

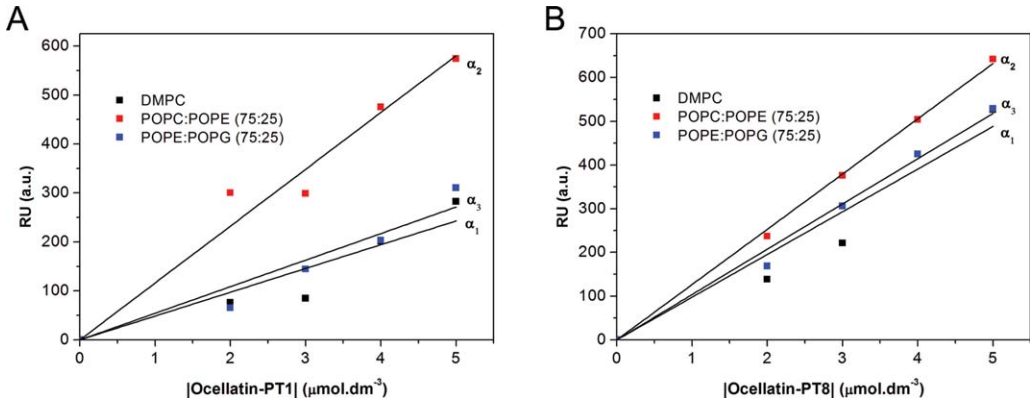

FIGURE 7 Dose–response relationship for the interaction of Ocellatin peptides with lipid films (DMPC, POPC:POPE 75:25, and POPE:POPG) from SPR data. The slopes of the lines fitted to this relationship (α) were (**A**) Ocellatin-PT1 ($\alpha_1 = 48.6$, $\alpha_2 = 116.1$, $\alpha_3 = 54.3$; (**B**) Ocellatin-PT8 ($\alpha_1 = 97.7$, $\alpha_2 = 126.4$, $\alpha_3 = 103.6$)

lipid bilayer followed by the peptide injection and finalizing with the lipid bilayer removal with CHAPS detergent. This cycle was repeated for each peptide concentration used. The sensorgrams obtained for the interactions of ocellatins-PT1 and PT-8 with the different model membranes used are depicted in Figure 6. The binding constants, calculated using the kinetic two-state reaction model, are listed in Table 2. For the mammalian cell mimetic liposomes (DMPC), K_{ass} was 2.95×10^3 for PT-1 and 2.18×10^4 for PT-8; for the bacterial cells mimetic liposomes [POPE:POPG (75:25)], K_{ass} was 1.03×10^5 for PT-1 and 1.28×10^6 for PT-8 and for the leishmania cells mimetic liposomes [POPC:POPE (75:25)], K_{ass} was 1.77×10^5 for PT1 and 1.94×10^5 for PT8. The sensorgrams in Figure 6 can also give information to make an analysis of the binding affinity at the equilibrium with a steady-state binding model. However, since we used anti-bacterial peptides that, at high concentration, are able to destroy the lipid membranes, we were forced to use a range of small concentrations and thus we were unable to reach the saturation concentration for these binding curves. Thus we measured a linear dose–response relationship at the equilibrium and the results are shown in Figure 7. The slopes of the linear plots are 48.6 for PT-1 and 97.7 for PT-8 with DMPC, 54.3 for PT-1 and 103.6 for PT-8 with POPE:POPG (75:25) and 116.1 for PT-1 and 126.4 for PT-8 with POPC:POPE (75:25). Overall, these results indicate a higher affinity of both PT-1 and PT-8 for bacteria and leishmania lipid membranes rather than mammalian lipid membranes.

4 | DISCUSSION

4.1 | Biological assays and morphological studies

To the best of our knowledge, this work represents the first time that a wide range of related peptides have been tested against antileishmania models.[28] The work showed that all the analyzed ocellatin-PT peptides are active against *Leishmania* promastigotes and some against amastigotes. Comparing with previous results of antibacterial activity tests,[15a] we observe slightly superior antiparasitic potency for the same peptides. Conversely, the peptides have low toxicity for macrophages confirming previous studies with other mammalian cells, a fact that may be related to differences in membrane composition between the mammalian and parasitic cells.

Microscopy results showed considerable morphological changes of *L. infantum* cells upon treatment with the

TABLE 2 Association (ka_1 and ka_2) and dissociation (kd_1 and kd_2) rate constants for interaction of the ocellatins with different membranes models, and affinity constants (K) determined by numerical integration using the two-state reaction model

Peptide name	Lipid type	ka_1 (1/mol.dm^{-3}s) $\times 10^3$	kd_1 (1/s) $\times 10$	ka_2 (1/s) $\times 10^3$	kd_2 (1/s) 10^{-4}	K (mol.dm^3) 10^3
Ocellatin-PT1	DMPC	0.212	2.36	3.51	15.5	2.95
	POPE:POPG (75:25)	4219	3.12	5.89	8.60	103
	POPC:POPE (75:25)	86.6	6.63	4.98	141	177
Ocellatin-PT8	DMPC	976	1.60	4.58	17.8	21.8
	POPE:POPG (75:25)	31.9	2.31	9.41	11.4	1279
	POPC:POPE (75:25)	17.5	1.77	4.20	43.5	194

ocellatin-PT1 and ocellatin-PT8. However, differences in morphological effects between the two peptides tested were not significant. Comparing image results with those previously published where considerable roughening of the membrane, shortening and rounding of the cells, as well as apparent changes to flagella was evidenced in promastigotes cells after treatment with DRS-01,[26] we observed more localized changes in promastigote cells after ocellatin-PT peptides treatment. The membrane itself showed visible but not significant roughening, while large blister-like protrusions appeared at lower concentrations and large holes in the membranes, some passing deep into the cell body, were observed at higher concentrations. It seems likely these are the result of the vesicalization/micellization of membrane lipids also observed at lower concentrations, and clearly represent a complete undermining of the membrane structure. In addition, at the lower concentration, the membranes showed dark patches (lower contrast) in some regions. This could be due to membrane thinning. Bearing in mind that this lower concentration was below the IC_{50}, while the higher concentration was above it, it seems likely that formation of vesicles and/or membrane thinning is a sub-lethal cell alteration caused by these peptides, while the penetration of the membranes illustrates effects that occur at a lethal concentration. It is clear from the literature,[27] that even among peptides which act directly on lipid membranes, the actual mechanism is a result of the combination of the specific peptide structure and the lipid composition of the membrane under study. Based on very different microscopy results, using the same parasite model, we conclude that the mechanisms of action of these new ocellatin-PT peptides is different to that of the DRS-01 previously described, which has a very distinct sequence compared to the ocellatins.[26]

4.2 | Structural studies, binding property of peptides to the lipid membrane, and comparison with bioactivity

The structural study of the ocellatin-PT peptides lead to the conclusion that these peptides most likely change their sstructure when they contact microorganism membranes, supporting the theory that the peptide interaction with the microorganism's membrane should be crucial for its activity, as demonstrated by AFM with leishmania (in this work) and with bacteria previously.[15a] However, there was no direct relation between the changes seen in systems with model membranes and the toxicity toward the modeled cell types. This could mean either that the simple models used are not adequate to fully probe secondary structures formed in contact with cells, or that for these peptides, alpha-helical structures are not a prerequisite for the mode of action.

Ocellatin-PT peptide interactions with different membrane models was then further investigated in this work using SPR, a technique that has been highlighted recently as one of the main biochemical techniques used to study molecular interactions.[29] The study of the binding of ocellatins PT-1 and PT-8 with different membrane models showed a higher affinity of both peptides for models for Gram-negative bacterial and leishmania membranes when compared to mammalian membranes. This correlates with previously described antibacterial tests and cytotoxicity studies, suggesting that the selectivity is based on membrane lipid composition.[15a] Anti-*L. infantum* and anti-*E. coli* IC_{50} and MIC concentrations were 24 $\mu mol.dm^{-3}$ and 300 μM respectively for ocellatin PT-1 and 15.5 $\mu mol.dm^{-3}$ and 60 μM respectively for ocellatin PT 8 while insignificant or null hemolytic and cytotoxicity activity were observed at the determined IC_{50} and MICs.

In brief, ocellatin-PT peptides present a solvent-dependent α-helix structure adoption that suggests a change in confirmation upon interaction with microorganisms. SPR studies demonstrate that peptides have preferential affinity for parasite and bacterial membrane models compared to the mammalian membrane model, this correlates with the *in vitro* activity tests performed in this work and previously with parasites, bacteria, human erythrocytes, murine fibroblast cells and bone marrow-derived macrophages. High-resolution microscopy techniques show peptide action through pathogen-membrane morphology alteration that could be due to membrane thinning and vesicle formation with final penetration provoking lysis. The mechanism of action is likely a result of the combination of the peptide structure and lipid composition of the membrane under study. Based on the cationic nature of these peptides, and the net positive charge of many bacterial membranes, the initial step in interaction is likely to be dependent on electrostatic interactions.[27] Similarly, electrostatic factors may explain their low cytotoxicity toward mammalian cells.[30] These results confirm the potential of ocellatin peptides to be used as therapeutic molecules due to high selectivity for microorganism membranes against mammalian membranes. The correlation of results between SPR, AFM and biological activity allows the conclusion that the use of biophysical techniques such as AFM and SPR enriches and complements the *in vitro* study of activity of peptides against microorganisms.

FUNDING INFORMATION

This work was partially supported by grants from INCT Nanobiotecnologia and PVE Project (MCT/CNPq), the *Consejo Nacional de Investigaciones Cientificas y Técnicas* (CONICET), and the *Agencia Nacional de Promoción Científica y Tecnológica* (ANPCyT). M.M.M. is a researcher at CONICET. This work has also been supported through project UID/MULTI/04378/2013-POCI/01/0145/FERDER/007728 with financial support from FCT/MEC through national funds and co-financed by FEDER, under the Partnership Agreement

PT2020. Scanning electron microscopy was carried out at *Centro de Materiais da Universidade do Porto*, CEMUP. Peter Eaton is supported by a *Ciência sem Fronteiras* grant via CNPq, and his lab work is supported by financial support from FCT/MEC through national funds and co-financed by FEDER, under the partnership agreement PT2020. Alexandra Plácido and Ana Georgina Gomes-Alves are grateful to FCT for their grants SFRH/BD/97995/2013 and SFRH/BD/93766/2013, financed by POPH–QREN–Tipologia 4.1–Formação Avançada, subsidized by *Fundo Social Europeu and Ministério da Ciência, Tecnologia e Ensino Superior*. Nuno Vale thanks Programa Operacional Regional do Norte (ON.2) and Faculdade de Ciências da Universidade do Porto (FCUP) for co-funding refurbishment of the Porto Peptide Synthesis Facility (POPUP) through operation NORTE-07-0162-FEDER000111. NV thanks Fundação para a Ciência e Tecnologia (FCT, Portugal) and FEDER (European Union) for funding through project grant IF/00092/2014. Work in AMT laboratory was supported by Project "NORTE-07-0124-FEDER-000002-Host-Pathogen Interactions" cofunded by Programa Operacional Regional do Norte under QREN, through FEDER and FCT. None of the funding bodies were involved in study design, in the collection, analysis and interpretation of data; in the writing of the report; or in the decision to submit the article for publication.

REFERENCES

[1] R. E. W. Hancock, G. Diamond, *Trends Microbiol.* **2000**, *8*, 402.

[2] X. Xu, R. Lai, *Chem. Rev.* **2015**, *115*, 1760.

[3] G. Wang, X. Li, Z. Wang, *Nucleic Acids Res.* **2009**, *37*, D933.

[4] a) G. D. Brand, R. C. Santos, L. M. Arake, V. G. Silva, L. M. Veras, V. Costa, C. H. Costa, S. S. Kuckelhaus, J. G. Alexandre, M. J. Feio, J. R. Leite, The skin secretion of the amphibian Phyllomedusa nordestina: a source of antimicrobial and antiprotozoal peptides. *Molecules* **2013**, *18*, 7058; b) Kuckelhaus, S. A. Leite, J. R. Muniz-Junqueira, M. I. Sampaio, R. N. Bloch, C. Jr.; Tosta, C. E. Antiplasmodial and antileishmanial activities of phylloseptin-1, an antimicrobial peptide from the skin secretion of Phyllomedusa azurea (Amphibia). *Exp. Parasitol.* **2009**, *123*, 11; c) Rivas, L. Luque-Ortega, J. R. Andreu, D. Amphibian antimicrobial peptides and Protozoa: lessons from parasites. *Biochim. et Biophys. Acta* **2009**, *1788*, 1570–81; d) Villa-Hernandez, O. Hernandez-Orihuela, L. del Carmen Rodriguez, M. Zamudio-Zuniga, F. Castro-Franco, R. Pando, V. Batista, C. V. Novel antimicrobial peptides isolated from skin secretions of the Mexican frog Hyla eximia. *Protein Peptide Lett.* **2009**, *16*, 1371.

[5] a) S. L. Cobb, P. W. Denny, *Curr. Opin. Invest. Drugs* **2010**, *11*, 868. b) de Moraes, J. Nascimento, C. Miura, L. M. Leite, J. R. Nakano, E. Kawano, T. *Chem. Biodiversity* **2011**, *8*, 548.

[6] H. W. Huang, *Biochemistry* **2000**, *39*, 8347.

[7] a) P. Eaton, P. West, *Atomic Force Microscopy*, Oxford University Press, Oxford, UK, **2016**; b) Mularski, A. Wilksch, J. J. Hanssen, E. Strugnell, R. A. Separovic, F, *Biochim. Et Biophys. Acta (BBA) - Biomembranes* **2010**, *1858*, 1091

[8] D. A. Phoenix, F. Harris, M. Mura, S. R. Dennison, *Prog. Lipid Res.* **2015**, *59*, 26.

[9] a) B. Pozo Navas, K. Lohner, G. Deutsch, E. Sevcsik, K. A. Riske, R. Dimova, P. Garidel, G. Pabst, *Biochim. Biophys. Acta.* **2005**, *1716*, 40. b) Zhao, W. Rog, T. Gurtovenko, A. A. Vattulainen, I. Karttunen, M. *Biochimie* **2008**, *90*, 930.

[10] A. H. Delcour, *Biochim. Biophys. Acta* **2009**, *1794*, 808.

[11] a) L. Zheng, R. T'Kind, S. Decuypere, S. J. von Freyend, G. H. Coombs, D. G. Watson, Profiling of lipids in Leishmania donovani using hydrophilic interaction chromatography in combination with Fourier transform mass spectrometry. Rapid Commun. Mass Spectrom. **2010**, *24*, 2074; b) Florin-Christensen, J. Suarez, C. E. Florin-Christensen, M. Hines, S. A. McElwain, T. F. Palmer, G. H. Phosphatidylcholine formation is the predominant lipid biosynthetic event in the hemoparasite Babesia bovis. *Mol. Biochem. Parasitol.* **2000**, *106*, 147; c) Retra, K. deWalick, S. Schmitz, M. Yazdanbakhsh, M. Tielens, A. G. Brouwers, J. F. van Hellemond, J. J. The tegumental surface membranes of Schistosoma mansoni are enriched in parasite-specific phospholipid species. *Int. J. Parasitol.* **2015**, *45*, 629; d) Riou, M. Grasseau, I. Blesbois, E. Kerboeuf, D. Relationships between sterol/phospholipid composition and xenobiotic transport in nematodes. *Parasitol. Res.* **2007**, *100*, 1125; e) Imbert, L. Ramos, R. G. Libong, D. Abreu, S. Loiseau, P. M. Chaminade, P. Identification of phospholipid species affected by miltefosine action in Leishmania donovani cultures using LC-ELSD, LC-ESI/MS, and multivariate data analysis. *Anal. Bioanal. Chem.* **2012**, *402*, 1169.

[12] M. Besenicar, P. Macek, J. H. Lakey, G. Anderluh, *Chem. Phys. Lipid* **2006**, *141*, 169.

[13] M. Suwalsky, M. Jemiola-Rzeminska, C. Astudillo, M. J. Gallardo, J. P. Staforelli, F. Villena, K. Strzalka, *Biochim Biophys Acta* **2015**, *1848*, 2829.

[14] A. C. Nascimento, L. C. Zanotta, C. M. Kyaw, E. N. Schwartz, C. A. Schwartz, A. Sebben, M. V. Sousa, W. Fontes, M. S. Castro, *Protein J.* **2004**, *23*, 501.

[15] a) M. M. Marani, F. S. Dourado, P. V. Quelemes, A. R. de Araujo, M. L. Perfeito, E. A. Barbosa, L. M. Veras, A. L. Coelho, E. B. Andrade, P. Eaton, J. P. Longo, R. B. Azevedo, C. Delerue-Matos, J. R. Leite, *J. Nat. Prod.* **2015**, *78*, 1495. b) Nascimento, A. Chapeaurouge, A. Perales, J. Sebben, A. Sousa, M. V. Fontes, W. Castro, M. S. *Toxicon* **2007**, *50*, 1095.

[16] J. M. Conlon, Y. H. Abdel-Wahab, P. R. Flatt, J. Leprince, H. Vaudry, T. Jouenne, E. Condamine, *Peptides* **2009**, *30*, 888.

[17] a) J. C. Sousa, R. F. Berto, E. A. Gois, N. C. Fontenele-Cardi, J. E. Honorio, Jr.; K. Konno, M. Richardson, M. F. Rocha, A. A. Camargo, D. C. Pimenta, B. A. Cardi, K. M. Carvalho, *Toxicon* **2009**, *54*, 23. b) Rollins-Smith, L. A. King, J. D. Nielsen, P. F. Sonnevend, A. Conlon, J. M. *Regulatory Peptides* **2005**, *124*, 173.

[18] P. Wolf, *Anal. Biochem.* **1983**, *129*, 145.

[19] B. Bjellqvist, B. Basse, E. Olsen, J. E. Celis, *Electrophoresis* **1994**, *15*, 529.

[20] J. Kyte, R. F. Doolittle, *J. Mol. Biol.* **1982**, *157*, 105.

[21] D. Sereno, J. L. Lemesre, *Antimicrob. Agents Chemother.* **1997**, *41*, 972.

[22] S. Vale-Costa, S. Gomes-Pereira, C. M. Teixeira, G. Rosa, P. N. Rodrigues, A. Tomás, R. Appelberg, M. S. Gomes, *PLoS Negl. Trop. Dis.* **2013**, *7*, e2061.

[23] M. S. Gomes, S. Sousa Fernandes, J. V. Cordeiro, S. Silva Gomes, A. Vieira, R. Appelberg, *Eur. J. Immunol.* **2008**, *38*, 2180.

[24] a) Whitmore, L. Wallace, B. A. Dichroweb. http://dichroweb.cryst.bbk.ac.uk/html/home.shtml (accessed: 9th July 2016); b) L. Whitmore, B. A. Wallace, *Biopolymers* **2008**, *89*, 392.

[25] N. Sreerama, R. W. Woody, *Anal. Biochem.* **2000**, *287*, 252.

[26] P. Eaton, C. R. Bittencourt, V. Costa Silva, L. M. Veras, C. H. Costa, M. J. Feio, J. R. Leite, *Nanomed. Nanotech. Biol. Med.* **2014**, *10*, 483.

[27] V. Teixeira, M. J. Feio, M. Bastos, *Prog. Lipid Res.* **2012**, *51*, 149.

[28] B. S. McGwire, M. M. Kulkarni, *Exp. Parasitol.* **2010**, *126*, 397.

[29] S. G. Patching, *Biochim. Biophys. Acta* **2014**, *1838*, 43.

[30] Y. Shai, Z. Oren, *Peptides* **2001**, *22*, 1629.

Reviewing Editor: David E. Wemmer

SUPPORTING INFORMATION

Additional Supporting Information may be found online in the supporting information tab for this article.